

Optimizing electrokinetic treatments for enhanced mortar durability: ionic migration and microstructural analysis

Priyanka Rajendran¹ , Revathi Vaiyapuri², Rajaiah Selvaraj³

¹Mookambigai College of Engineering, Department of Civil Engineering, 622502, Keeranur, Pudukkottai, Tamilnadu, India.

²KSR College of Engineering, Department of Civil Engineering, 637215, Namakkal, Tamilnadu, India.

³Civil Material testing Laboratory, CSIR-CECRI, 630 006, Karaikudi, Tamilnadu, India.

email: drpriyankarajendran@gmail.com, revthiru2002@yahoo.com, selvarajcecri@gmail.com

ABSTRACT

This study investigated the effects of electrokinetic treatments on mortar specimens using a range of experimental techniques. Ionic migration tests revealed that increasing voltage and duration led to higher charge transfer, with $\text{Ca}(\text{OH})_2$ electrolyte showing the highest cationic migration. X-ray fluorescence analysis indicated that Nano-Silica treatment resulted in the highest oxide content, transforming absorbed elements effectively. The chloride penetration test demonstrated that $\text{Ca}(\text{OH})_2$ treatment exhibited the lowest charge passed, suggesting minimal chloride penetration, while NaOH and KOH treatments showed higher charge passed. Field Emission Scanning Electron Microscopy analysis provided visual evidence of structural changes and material depositions. Calcium Hydroxide treatment reduced porosity, Sodium Hydroxide, and Potassium Hydroxide treatments displayed distinct particle distributions, and Nano Silica treatment led to the formation of hair-like crystal structures. These findings help to understand the microstructure and composition of cement mortar specimens after various treatments. The nano-silica electrolyte appeared as a viable choice for electro-kinetic therapy, whereas $\text{Ca}(\text{OH})_2$ treatment stated the potential to reduce chloride penetration in mortar specimens. The results offer insights into optimizing electrokinetic treatments for improved mortar performance.

Keywords: Electrokinetic treatments; Mortar; Ionic migration; Nano-Silica treatment; Chloride penetration.

1. INTRODUCTION

Durability is the principal concern of Civil engineers today. Electrokinetic technique is a very recent and effective technique for enhancing the durability of Cement Mortar [1]. The surface defects and corrosion can be treated in many ways such as Epoxy injection, Polymer impregnation, Stitching, Drilling, and Plugging, which are the recent techniques for curing the crack [2, 3]. Rather than curing the crack, it can be prevented by increasing strength and stiffness, improving durability, improving the concrete surface's appearance, providing water tightness, and Corrosion protection, Increased strength, and stiffness can be achieved by using electro Electro-kinetic technique [4]. Using the Electro-kinetic technique, the pores in the mortar are Blocked or Clogged with ions [5]. This results in enhanced Durability of Mortar as the pore water ingress is avoided.

ALLISON *et al.* [6], demonstrated precipitating polymorphs of calcium carbonate template 3-D. The study focused on depositing calcium carbonate in porous materials using electromigration. The duration and applied potential were varied. X-ray diffraction and SEM study were done for the determination of polymorph formation. The morphology was also studied. The results showed that shorter durations and higher potentials are more effective information of Calcium Carbonate of meta-stable polymorphs with porous media infill [7, 8]. These results are useful in medical and structural applications for the development of bio-inspired composites. MOREFIELD *et al.* [9] explored two new approaches that can produce new composites. These composites consist of both electrophoretically infiltrated particulates and cementing reactions will be present which can help in binding the particulates. In this approach, using electro-transport nano-sized particles were made to migrate into pores of Concrete or Mortar and produce a cementing reaction inside. And thus, a new composite is formed. The first set of Mortar samples was infiltrated with nanoparticle silica fume and sodium silicate was used as a cementation reaction. In the second set, nanoparticle silica fume was used for treatment and a sodium silicate for cementation reaction. In the third set infiltration using calcium carbonate nano-sized crystals and calcium carbonate was the cementation reaction [10]. The best results were shown by silica-based and

carbonate-based infiltration systems. It worked to the extent that the treated density was greater than the initial density. CARDENAS *et al.* [11] suggested the employment of Electro Kinetic nanoparticle treatment for the mitigation of corrosion. To the reinforcement via capillary pores of concrete, pozzolanic nanoparticles were driven under an electric field. This was done to prevent chlorides and sulphates penetration into Concrete. Both freshly batched and mature Concrete was studied. For the freshly batched Concrete specimens with EN treatment, the corrosion rate was reduced by a factor of 74 when compared to the untreated control [12]. For mature specimens, corrosion of untreated was 8 times that of treated specimens. As per the study, it was evident that using Electro Kinetic nanoparticle treatment, the pH and chloride content was effectively minimized for both mature and young Concrete. DEPAOLI *et al.* [13]., experimented with the decontamination of Concrete using Electro Kinetics. A lixiviant solution is kept in contact with contaminated Concrete with the application of an electric field. It was found that among the contaminants, which are non-precipitating type are easy to be transported out of Concrete using Electro Kinetics. Using Electro Kinetics, Cesium, and strontium were transported through Concrete with lixiviants as electrolyte solutions. But decontamination of Concrete which contains precipitating species was found to be slow and troublesome using Electro Kinetics. KIM *et al.* [14], reported that the marine clay adjacent to the offshore foundation has become an electrokinetic technique for strengthening. This process was treated with four electrodes and an applied voltage is 6.2V. The vane shear strength and water penetration test were determined in this process [15]. The shear strength is increased in marine clay during electro-kinetic treatment. SANDEEP *et al.* [16]., have reported the results of an experimental study conducted on Cochin marine clay to evaluate the electro-kinetic treatment to increase shear strength [17]. RANJITHA *et al.* [18]., dealing with the application of chemical ground improvement techniques using the electro-kinetic process. CARDENAS *et al.* [19] ARUTSELVAM *et al.* [20], reported the application of chemical ground improvement using the electro-kinetic stabilization (EKS) method has the potential to overcome problems in soft compressibility soil. HSIEH *et al.* [21], investigated the use of Electro-Kinetic (EK) techniques and geotextiles to dehydrate high-water content sludge obtained from a local watershed reservoir. ARTI ALOK *et al.* [22], reported the effect of anode solution pH on the electro-osmosis process of electro-kinetic remediation of cadmium-contaminated soil at a wide range of pH (pH 3-12). By incorporating pozzolana, the resistance of the concrete to chemical intrusion is enhanced, particularly against chlorides or sulfates, resulting in improved performance in the presence of these substances.

The work methodology shows the process that has been carried out in this research. The process includes Electro-kinetic treatment, evaluation of durability by chloride ion penetration test, the study of mechanical properties, corrosion study, and microstructural study. The novelty of the project is to enhance the durability of cement mortar and Corrosion protection by the Electro-kinetic method by pores and defects filling with ionic migration. Different electrolytic solutions were used for the study. The best electrolytic solution was evaluated from Potassium Hydroxide (KOH), Sodium Hydroxide (NaOH), Calcium Hydroxide (Ca(OH)₂), and Nano Silica [23-25]. The durability of cement mortar is tested by Electro-kinetic treatment and the potentials used for the study are 6V, 12V, 18V, and 20V with varying durations of 4 hours, 6 hours, and 8 hours. The results were compared regarding the strength aspect and durability aspects. To improve the Durability of Cement Mortar by inducing the Electro-Kinetic principle through Pore filling effect due to the Ionic migration by Electro-Kinetic concepts. The study highlights the novel application of Nano-Silica electrolyte for electrokinetic therapy in cement mortar specimens, showing enhanced oxide content and the formation of unique hair-like crystal structures, providing valuable insights for optimizing mortar performance.

2. MATERIALS AND SAMPLE PREPARATION

The specimens were created using Portland Pozzolana Cement (PPC) in accordance with the guidelines specified in IS 1489 (Part I) 1991 for fly ash-based cement. PPC is produced by combining OPC clinker with 15 to 35% pozzolanic materials and the necessary amount of gypsum. These pozzolana are siliceous substances that can be added to concrete mixtures without compromising their performance characteristics [26]. However, it should be noted that the presence of pozzolana may lead to a slower curing rate compared to OPC, resulting in lower early strengths than OPC-based concrete [27]. Nonetheless, over time, the strength of PPC-based concrete can surpass that of OPC-based concrete. Utilizing pozzolana as a matrix binder for agglomeration offers several advantages, including cost-effectiveness, environmental friendliness, increased liquid absorbency, and the production of highly durable concrete. To ensure the quality of the river sand used, it undergoes screening and washing processes to remove any organic or inorganic compounds that may be present [28]. The sand used in this context has been sieved to retain particles passing through a 4.15mm sieve and retained on a 600µ sieve as fine aggregate. According to the specifications outlined in IS: 3025 (Part 21)-2009, the water used for concrete mixing and curing should be free from harmful substances [29]. Potable water is considered suitable for this purpose. These copper plates were embedded in mortar specimens to serve as cathodes (Figure 1). Additionally, square-shaped meshes made of aluminum plates were cut to act as anodes. These aluminum plates function as

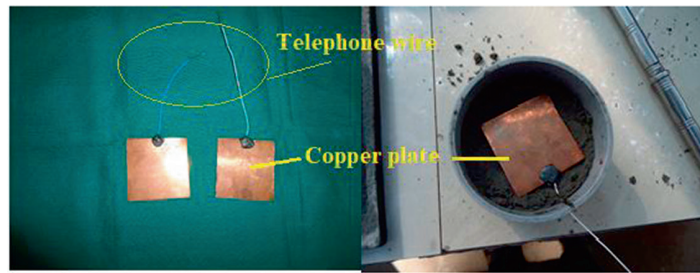


Figure 1: Copper plate with telephone wire.

electrodes, which are conductive elements used to establish contact with nonmetallic parts of a circuit. Electrodes play a crucial role in providing current through nonmetal objects to induce various changes and measure conductivity. Calcium hydroxide, potassium hydroxide, sodium hydroxide, and nano-silica were selected as electrolyte solutions.

3. EXPERIMENTAL STUDY

3.1. Cationic migration test

For a quick assessment of the mortar’s resistance to cation ion penetration, this test measures the electrical conductance of the material. The test procedure involves measuring the amount of electrical current flowing through disc specimens measuring 83 mm in diameter and 50 mm in depth, as well as specimens measuring 60 mm in diameter and 120 mm in depth, during the course of four, six, and eight hours [30-32]. One specimen is submerged in a solution of calcium hydroxide, potassium hydroxide, sodium hydroxide, and nano-silica, while the other three are immersed in calcium hydroxide, potassium hydroxide, and sodium hydroxide.

It has been observed that the total charge passed, expressed in coulombs, is correlated with the specimen’s resistance to cation penetration. For approximately 4 hours, 6 hours, and 8 hours, the current is monitored and recorded as indicated in Figure 2, every 30 minutes. The charge passed can also be computed by using Simpson’s rule as given in Equation 1. The charge passed is expressed in coulombs.

$$Q = 900x(I_0 + 2I_{30} + 2I_{60} + \dots + I_{360}) \tag{1}$$

Q – Charge Passed (Columns)

I₀ – Current immediately after voltage is applied

I_{final} – Current at final after voltage is applied

The value for the total charge passed must be changed if the specimen diameter is less than 95 mm. By multiplying the ratio of the cross-sectional areas of the standard and the actual specimens as stated in Equation 2, the adjustment is made.

$$Q_s = Q \left(\frac{95}{x} \right)^2 \tag{2}$$

Where,

Q_s – Charge passed (Columns) through 95 mm diametere speciemen

Q – Current passed through adjustable diametere speciemen

X – Diametre of the nonstandard specimen

3.2. X-ray fluorescence (xrf) analysis

When a material has been stimulated by being bombarded with high-intensity X-rays or gamma rays, it emits characteristic “secondary” (or fluorescent) X-rays. Ionization of the constituent atoms of materials is possible when they are exposed to short-wavelength X-rays or gamma rays [33, 34]. When an atom is exposed to radiation with an energy higher than its ionization potential, it may ionize, which is the process by which one or more electrons are ejected from the atom. It is possible for X-rays and gamma rays to have energy levels high



Figure 2: Cationic migration test.

enough to forcefully remove electrons from an atom’s inner orbital [35]. When one electron is removed in this fashion, the atom’s electronic structure becomes unstable, and electrons from higher orbitals “fall” into lower orbitals to fill the gap that is left. A photon is released as a result of falling, and its energy is equal to the energy difference between the two orbitals involved. As a result, radiation from the material has the energy of the atoms it contains. The term “fluorescence” refers to phenomena where radiation of a certain energy is absorbed and then re-emitted at a different energy that is typically lower. The HORIBA Scientific XGT 520 from Japan is the manufacturer of the XRF instrument.

3.3. Rapid chloride ion diffusion test (astm c 1202-94)

To quickly determine a mortar’s resistance to chloride ion penetration, the test procedure includes measuring its electrical conductance after being electro-kinetically treated. The test method entails measuring the quantity of electrical current that flows through disc specimens that are 83 mm in diameter and 50 mm deep over the course of six hours. The chloride ion permeability table according to ASTM C-1202 is shown in Table 1. A 60-volt direct current is applied across a cement specimen immersed in a 3.5% sodium chloride solution on one end and a 0.1 M sodium hydroxide solution on the other end [36]. The charge passed in Coulombs is correlated with the permeability of chloride ions into the specimen. The negative terminal of the power supply is connected to the NaCl solution cell, while the positive terminal is connected to the NaOH solution cell [37]. This setup allows for the investigation of the chloride penetration process and its relationship to the applied voltage. A 60-volt direct current is applied once the specimen has been fixed in the cell and the solution has been added. An ammeter is used to measure the starting current at the time the test is started, or when the power supply is turned on. The temperature of the solution in each cell is measured and recorded every 30 minutes for a total of 6 hours. The test must end when the temperature reaches 90°C at any point prior to the 6-hour completion window. Particularly when there is considerable chloride permeability, this happens. The charge passed can be calculated by plotting current versus time. The area under the curve will indicate the charge passed. Figure 3 depicts this test.

If the diameter of the specimen is more than 3.75 inch (95mm), the ‘e’ value for the total charge transmitted must be modified. The measurement is performed by multiplying the value obtained above the ratio of the cross-sectional area of the standard and real specimens as provided in Equation 3. The factors that are known to affect the chloride ion penetration include water-cement ratio, presence of polymeric admixtures, age of specimens, air voids system, and aggregate type.

Table 1: Chloride ion permeability according to ASTM C-1202.

CHARGE PASSED (COULOMBS)	CHLORIDE ION PERMEABILITY
<100	Negligible
100 – 1000	Very low
1000 – 2000	Low
2000 – 4000	Moderate
> 4000	High



Figure 3: Setup of chloride ion penetration test.

$$Q_s = Q \left(\frac{3.5}{x} \right)^2 \quad (3)$$

Where,

Q_s – Charge passed through 3.75 inch (95 mm) diametere speciemen

Q – Charge passed through y inch diametere speciemen

X – Diametre of the standard speciemen

3.4. Field emission scanning electron microscopy (FESEM)

A field emission cathode in the SEM generates narrower probing beams, improving spatial resolution and reducing sample charging and damage. The FESEM, produces clearer and less distorted images caused by electrostatic forces, achieving an exceptional resolution as low as 1.5 nm. This resolution is three to six times superior to that of traditional SEM. Furthermore, the FESEM enables the examination of smaller contamination spots using electron-accelerating voltages that are compatible with energy-dispersive X-ray spectroscopy [38]. By reducing the penetration depth of low kinetic energy electron probes, it allows for close inspection of the immediate surface of the material. The FESEM also produces high-quality images at low voltages while minimizing sample charging. Manufactured by ZEISS SUPRA-55 VP in Germany, this instrument significantly reduces the necessity for applying conductive coatings on insulating materials [39]. The FESEM is used for investigating construction details, precise coating thickness determination, contamination feature measurement, and elemental composition analysis with voltages ranging from 0.5 to 30 kV.

4. RESULTS AND DISCUSSION

4.1. Cationic migration test

With the aid of plastic vessels in which a circular specimen with a stainless-steel mesh implanted centrally with an electric lead was installed, an ionic migration test was performed on mortar specimens. The stainless-steel anodes (-ve) plates are positioned on either side of the circular disc, according to the size of the specimens. The positive terminals of these two plates are connected units [35, 36]. NaOH, KOH, Nano Silica, and $\text{Ca}(\text{OH})_2$ were chosen as the electrolytes. The electrical ends are linked to a DC power source, and for each test, voltages of 6, 12, 18, and 20 volts were applied for 4, 6, and 8 hours, respectively. Ionic motions begin once the power supply source is turned on. Nano Silica solutions were made with 1.5 grams of Nano Silica powder in 1 litre of water and were prepared with saturated $\text{Ca}(\text{OH})_2$, 0.1 M NaOH, and 0.1 M KOH electrolytic solution concentrations. The polarity was altered for the Nano Silica electrolyte. Every half-hour during the test, the circuit current in each cell was monitored in order to calculate the cationic charge that was passed into the specimen. Table 2 presents the cationic charge that was transferred during the experiment.

1. It was found that all electrolytic solutions gradually increased in charge passed when the voltage was raised from 6V to 20V.
2. Charge passed increased for all electrolyte solutions as the time the voltage was applied increased from 4 hours to 8 hours.

Table 2: Cationic migration.

ELECTROLYTIC SOLUTION	DURATION (HOUR)	CHARGE PASSED (COULOMBS)							
		CATIONIC MIGRATION				CATIONIC DIFFUSION			
		6V	12V	18V	20V	6V	12V	18V	20V
Ca(OH) ₂	4	719	2263	15896	4503	2405	2880	15896	6130
	6	1615	4668	17867	7840	3281	3957	17867	14534
	8	2675	7026	18682	11306	6400	8579	18682	16616
KOH	4	660	1544	11841	2304	2800	3092	11841	6023
	6	1615	3431	12685	5399	3118	4209	12685	7633
	8	2452	5057	15859	8517	5899	5834	15859	14356
NaOH	4	1143	5116	11802	3513	3597	2685	11802	4156
	6	2209	6371	12045	6802	6278	3481	12045	5873
	8	2294	4894	14673	8071	4721	4951	14673	7849
Nano Silica	4	143	1072	1696	1250	424	1279	1696	1911
	6	228	1992	1743	2594	814	1465	1743	2394
	8	262	2075	1963	3997	1173	1534	1963	2504

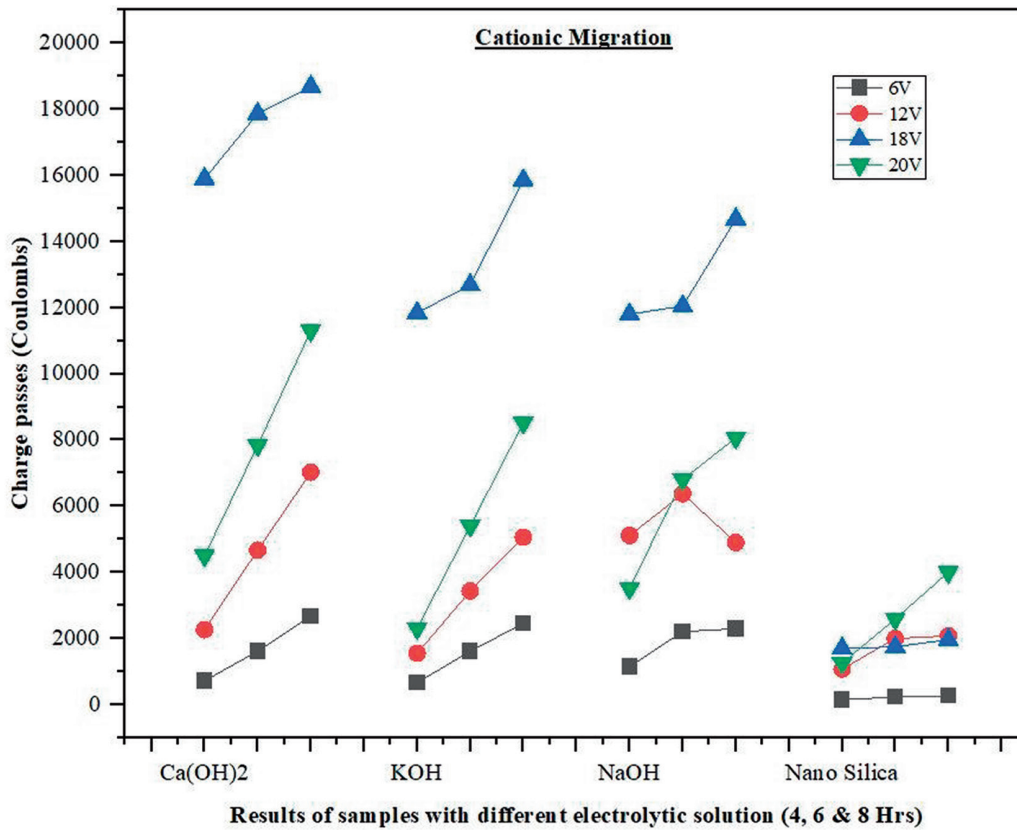


Figure 4: Rate of cationic migration with different timing.

When a 20V power supply was used for 8 hours, it was observed that the most charge was passing through an electrolytic cell. This finding indicates that the highest number of cations can flow through at the maximum voltage and time. The cations that penetrated the specimens the fastest were Ca ions, sodium ions, potassium ions, and finally nano-silica. The results match the ions' sizes as shown in the table quite well. The increased diffusion of Ca ions can be explained by Ca⁺⁺ smaller ionic radius relative to other ions. K⁺ strong mobility is a result of its unity valency, despite the fact that its ionic radius is a little bit greater. Slower mobility is displayed by nano-silica, also known as SiO₂. Therefore, Ca(OH)₂ electrolyte produces 11,306 coulombs, the highest cationic migration for the disc specimens. Following this, during a 20V-8-hour period, are Nano Silica with 3997 coulombs, NaOH with 8571 coulombs, KOH with 8017 coulombs, and KOH without Nano Silica. Figure 4 shows

the graphical representations of the cationic migration. Ca(OH)₂ electrolyte has the highest cationic migration for the cylindrical lollipops, which is 16,616 coulombs. With a 20V-8-hour period, NaOH comes next with 14,356 coulombs, KOH comes next with 7,849 coulombs, and Nano Silica comes last with 2,504 coulombs. Figure 5 contains the graphical representations of the cationic diffusion.

4.2. X-ray fluorescence (XRF)

The “Horiba” Machine from Japan was used to do X-ray fluorescence analysis on powder samples. XRF analysis is better for identifying the chemical composition. The samples were exposed to a 20V DC for eight hours and included control samples, specimens treated with Ca(OH)₂, Nano Silica, KOH, and NaOH. Table 3 displays

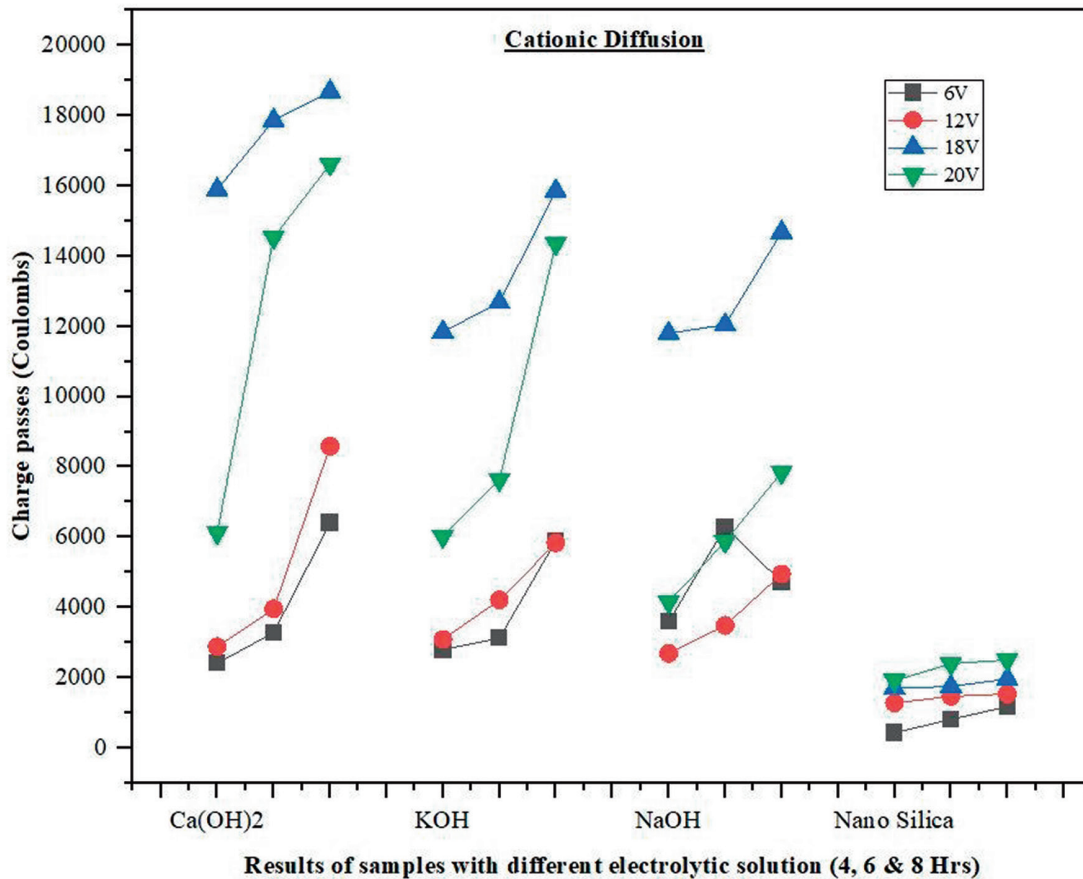


Figure 5: Rate of cationic diffusion with different timing.

Table 3: Oxide composition of materials by XRF analysis.

SPECIMEN	CONTROL	CA(OH) ₂	NAOH	KOH	NANO SILICA
Ca ²⁺	37.026	34.389	37.515	38.345	32.215
CaO	51.806	48.117	52.491	53.652	45.076
Si ⁻	13.008	9.124	11.433	8.600	16.533
SiO ₂	27.827	19.518	24.458	18.396	35.367
Fe ²⁺	10.960	11.644	9.192	16.339	10.843
Fe ₂ O ₃	15.670	16.648	13.142	23.360	15.503
K ⁺	Trace	7.340	1.018	0.449	0.793
K ₂ O	Trace	8.842	1.227	0.540	0.956
Element mass percentage (%)	-	53.373	47.725	55.133	48.748
Oxide mass percentage (%)	-	93.925	91.318	95.948	96.902

the analysis's findings with an emphasis on element and oxide composition. The table shows that the absorbed elements changed into oxide form in the presence of oxygen after the electrokinetic research. Figures 6 to 10 shows the corresponding values. Notably, the specimens that had been treated with Nano-Silica showed the greatest oxide content (96.902%), making it the most successful treatment. The specimens that had been

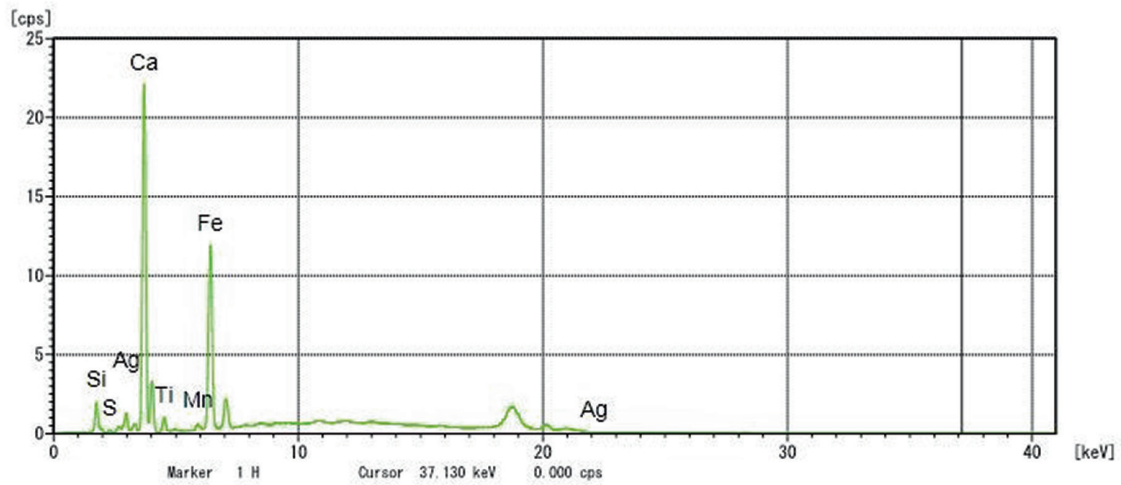


Figure 6: XRF analysis for control specimen.

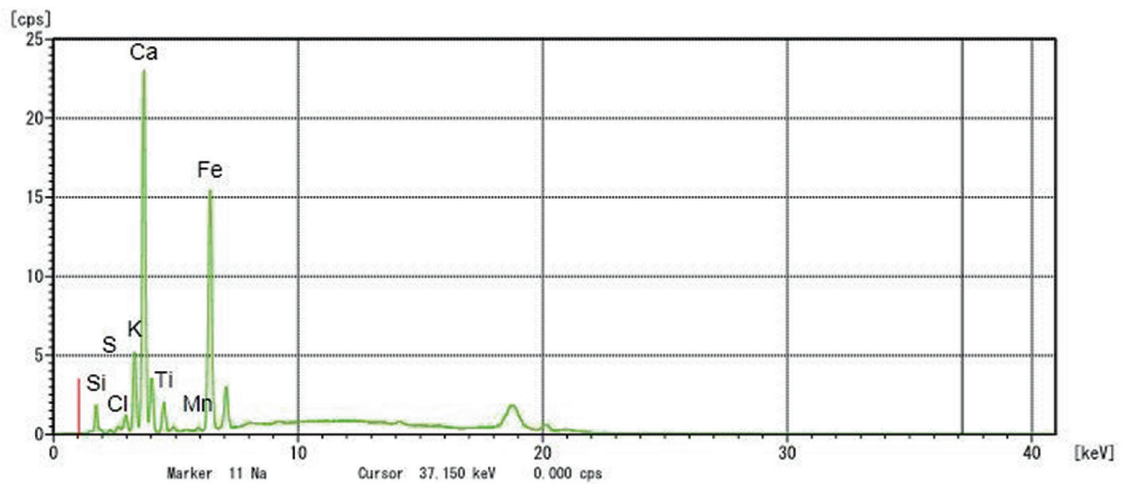


Figure 7: XRF analysis for Ca(OH)₂ treated specimen.

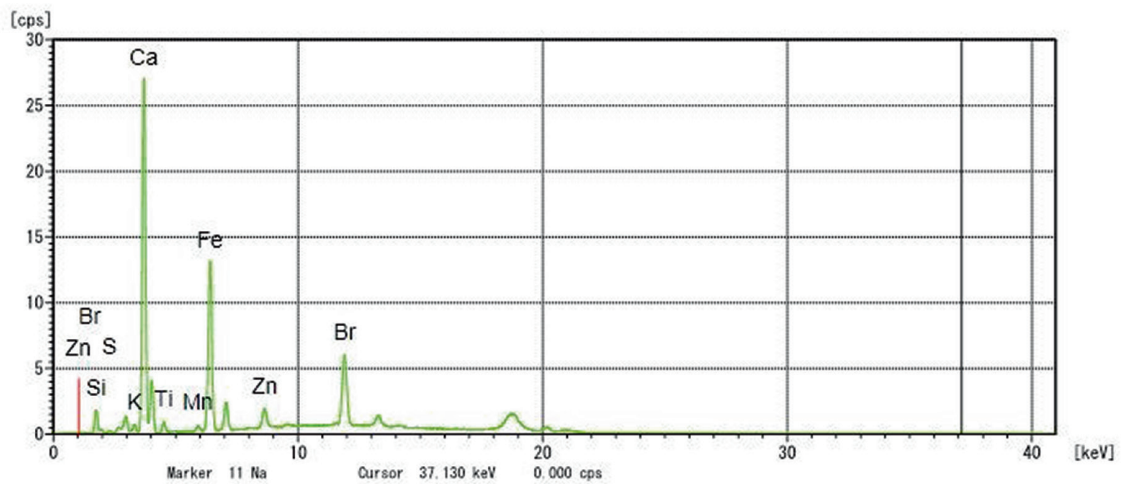


Figure 8: XRF analysis for NaOH treated specimen.

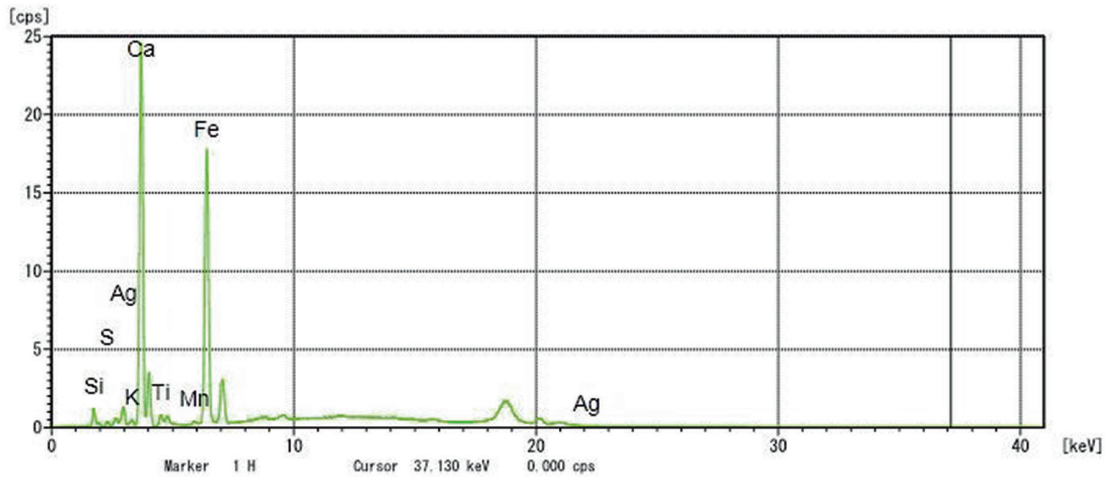


Figure 9: XRF analysis for KOH treated specimen.

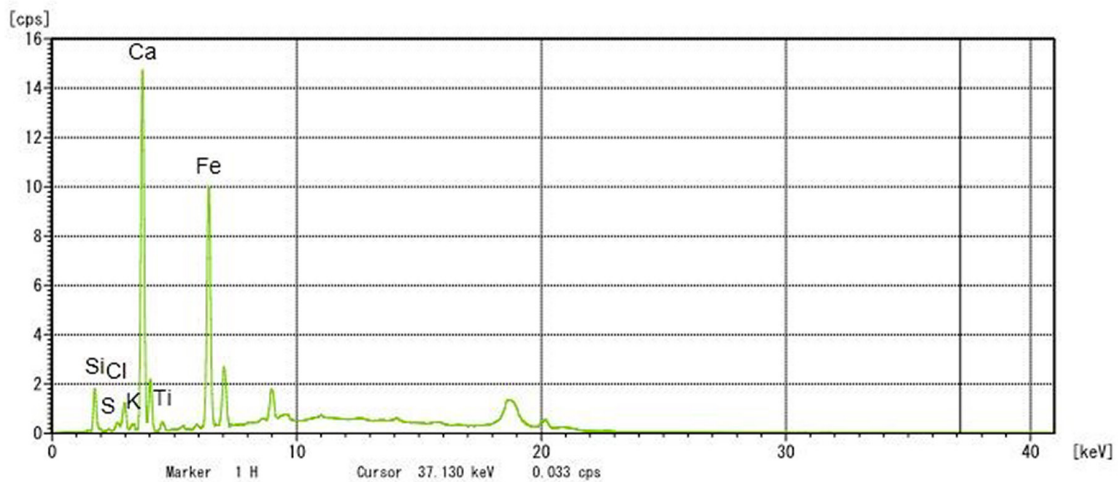


Figure 10: XRF analysis for Nano Silica treated specimen.

exposed to NaOH attained an oxide composition of 91.318%, placing them in second place. KOH came in second place with an oxide composition of 95.748%. Because of its nano size and high penetration capacity of 35.367%, Nano Silica exhibits outstanding performance in mortar specimens with voids, capillaries, fissures, and cracks that are difficult to reach with other materials. According to this study, Nano-Silica electrolyte is the most efficient for Electro Kinetic therapy.

4.3. Chloride diffusion test (ASTMC 1202-12)

This test is conducted using specially designed PVC cells, with a cement mortar specimen placed between two containers as depicted in the figure. The purpose of the test is to determine the amount of charge that is transferred into the specimen or the extent of chloride penetration. One of the cells contains a 3.5% NaCl solution, while the other cell is filled with a 0.1M NaOH solution. Titanium mesh electrodes are placed inside both cells. A constant electric current of 60 volts DC is applied using a power supply source with a capacity range of 0-60 volts DC and 0-5 amps. The negative terminal of the power supply is connected to the NaCl solution, while the positive terminal is connected to the NaOH solution. Once the power supply is switched on, a stable 60 volts DC is applied to the system, and the corresponding electric circuit current is measured. Multiple cells can be connected simultaneously, typically around 6 to 8 cells, as long as the total integrated current does not exceed 4 or 4.5 amps to ensure safe operation. The test duration is set at six hours, during which the circuit current is measured for each individual cell. These measurements are taken at regular intervals, usually every half an hour, to monitor the changes in the electric current over time. By analyzing the recorded data, it is possible to assess the quantity of charge passing through the specimen or the extent of chloride penetration into the specimen throughout the test period.

The computed charge passed in coulombs, as presented in Table 4, provides a quantitative assessment of the test results regarding chloride penetration in the cement mortar specimens. The test setup, depicted in Figure 11, facilitated the evaluation of different treatments. Upon analyzing the data, it becomes evident that the $\text{Ca}(\text{OH})_2$ treated sample displayed the lowest charge passed, indicating minimal chloride penetration. This outcome aligns with the observed behavior in the cationic diffusion cell, where Ca^{++} ions exhibited greater penetration, effectively obstructing the entry of chloride ions by blocking pores, voids, and fissures. The NaOH treated specimens ranked second in terms of charge passed, indicating a relatively higher level of chloride penetration compared to the $\text{Ca}(\text{OH})_2$ treated samples. The KOH-treated specimens followed in third place, showing a similar trend but with a slightly higher charge passed. The specimen treated with nano silica exhibited the highest charge passed, suggesting a greater degree of chloride penetration. This result can be attributed to the limited mobility of SiO_2 molecules within the cationic diffusion test. Thus, the findings from the computed charge passed measurements correspond well with the observations made in the cationic diffusion cell experiments. The $\text{Ca}(\text{OH})_2$ treatment

Table 4: Chloride penetration test results.

ELECTROLYTIC SOLUTION	DURATION (HOUR)	CATIONIC DIFFUSION			
		CHARGE PASSED (COULOMBS)			
		6V	12V	18V	20V
$\text{Ca}(\text{OH})_2$	4	710	509	496	218
	6	594	463	403	121
	8	495	334	267	417
KOH	4	686	564	519	315
	6	573	496	463	208
	8	517	412	392	368
NaOH	4	663	516	473	276
	6	516	427	394	179
	8	418	268	247	469
Nano Silica	4	718	578	508	393
	6	598	411	302	264
	8	484	309	299	344



Figure 11: Chloride diffusion test.

proved to be effective in reducing chloride penetration, while the Nano Silica treatment resulted in increased chloride penetration due to the constrained mobility of SiO_2 molecules. These results contribute to our understanding of the mechanisms involved in chloride penetration and the influence of different treatments on the permeability of cement mortar specimens.

4.4. Field emission scanning electron microscopy

FESEM (Field Emission Scanning Electron Microscopy) testing was conducted on all specimens, and images were obtained to examine the effects of electro-kinetic treatment. The FESEM test results provided clear visual evidence of ion deposition from the electrolyte during treatment. Various magnifications were employed to capture detailed FESEM images, with WD representing the working distance between the lens and the specimen, and EHT denoting the voltage used to accelerate electrons. In the obtained FESEM images, different particle structures, and materials were identified. Conductive materials appeared as white and bright particle images, while non-conductive mediums appeared dark. The particle structures could be easily visually identified from these images. The untreated specimen image in Figure 12a revealed visible pores and voids, with occasional

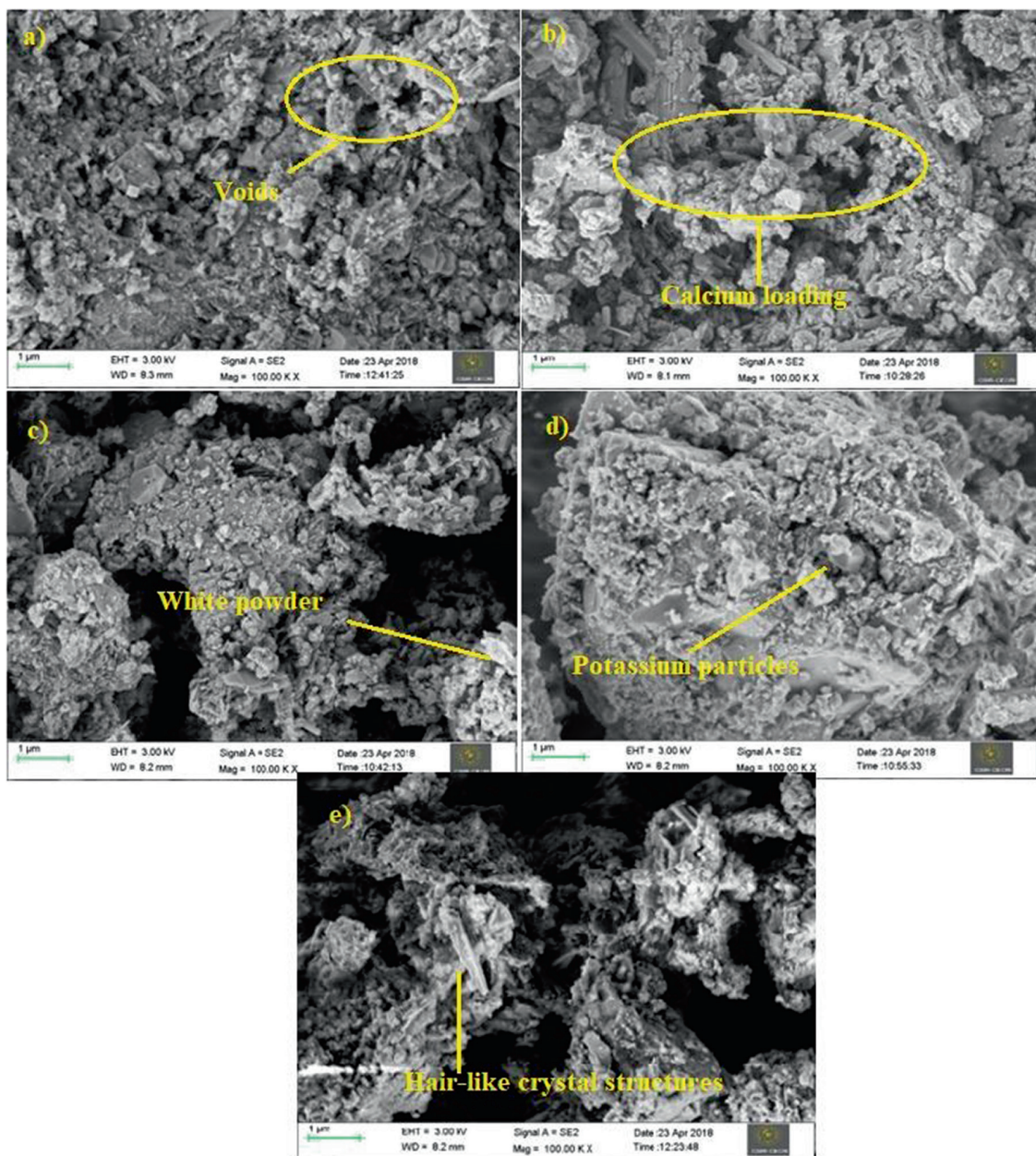


Figure 12: (a) Untreated specimen, (b) Ca(OH)_2 treated specimen, (c) NaOH treated specimen, (d) KOH treated specimen, (e) Nano Silica treated specimen.

dark areas indicating larger pores or voids. In the FESEM images of the Calcium hydroxide-treated specimen (Figure 12b), a reduction in porosity was observed. This reduction was attributed to the loading of Calcium into the mortar's pores. Free calcium likely reacted with silica in the matrix, resulting in the sealing of pores. For the Sodium hydroxide-treated specimen, various magnified images (Figure 12c) showed the presence of white powder patches. No expected reactions were anticipated between the sodium particles penetrating the specimen and the mortar matrix. Similarly, white powder patches were observed in the FESEM magnified images of the Potassium hydroxide-treated specimens (Figure 12d). These patches indicated the penetration of Potassium particles into the Cement Mortar surfaces. The FESEM images of the Nano Silica treated specimens (Figure 12e) revealed the formation of hair-like crystal structures. This formation was attributed to the reaction between Calcium Hydroxide present in the mortar and Nano Silica, leading to the sealing of pores. A Ca-SiO₂ chain network was formed, and the formation of C-S-H gel within the matrix was expected. In conclusion, the FESEM analysis provided valuable insights into the structural changes and material depositions resulting from the electrokinetic treatments. The images confirmed the reduction in porosity for the Calcium Hydroxide treated specimen, while the Sodium Hydroxide and Potassium Hydroxide treated specimens showed distinct particle distributions. The Nano Silica treated specimens exhibited the formation of unique hair-like crystal structures. These observations contribute to a better understanding of the effects of different treatments on the microstructure and composition of the cement mortar specimens.

5. CONCLUSION

The key findings of this study have been summarized as follows:

1. The ionic migration test on mortar specimens revealed that increasing the voltage and duration of application resulted in an increase in the charge passed for all electrolyte solutions. The highest cationic migration was observed with Ca(OH)₂ electrolyte, followed by Nano Silica, KOH, and NaOH. The results were consistent with the ions' sizes and valencies, with Ca ions exhibiting the fastest mobility.
2. The X-ray fluorescence analysis on powder samples treated with different electrolytes revealed that Nano-Silica treatment resulted in the highest oxide content (96.902%), indicating its effectiveness in transforming absorbed elements into oxides. NaOH and KOH treatments also showed significant oxide compositions (91.318% and 95.748% respectively). Nano Silica, with its small size and high penetration capacity, demonstrated excellent performance in reaching cracks, capillaries, and voids in mortar specimens. Therefore, the study suggests that Nano-Silica electrolyte is the most efficient option for Electro Kinetic therapy.
3. The chloride penetration test using PVC cells and different treatments revealed that Ca(OH)₂ treatment resulted in the lowest charge passed, indicating minimal chloride penetration. NaOH and KOH treatments showed higher charge passed, while Nano Silica treatment exhibited the highest charge passed due to limited mobility. These findings align with observations in the cationic diffusion cell experiments, providing insights into the mechanisms and permeability of cement mortar specimens regarding chloride penetration.
4. The FESEM analysis of the electrokinetically treated specimens revealed significant structural changes and material depositions. The Calcium Hydroxide treatment reduced porosity through the loading of Calcium into the mortar's pores. Sodium Hydroxide and Potassium Hydroxide treatments showed distinct particle distributions. The Nano Silica treatment resulted in the formation of hair-like crystal structures, indicating the reaction between Calcium Hydroxide and Nano Silica. These findings enhance our understanding of the microstructural effects of different treatments on cement mortar specimens.

6. BIBLIOGRAPHY

- [1] MARTINEZ, I., CASTELLOTE, M., "Preliminary study of the influence of supplementary cementitious materials on the application of electro remediation processes", *Materials (Basel)*, v. 14, n. 20, pp. 6126, 2021. doi: <http://dx.doi.org/10.3390/ma14206126>. PubMed PMID: 34683714.
- [2] SHAN, H., XU, J., WANG, Z., *et al.*, "Electrochemical chloride removal in reinforced concrete structures: improvement of effectiveness by simultaneous migration of silicate ion", *Construction & Building Materials*, v. 127, pp. 344–352, 2016. doi: <http://dx.doi.org/10.1016/j.conbuildmat.2016.09.137>.
- [3] PATTUSAMY, L., RAJENDRAN, M., SHANMUGAMOORTHY, S., *et al.*, "Confinement effectiveness of 2900psi concrete using the extract of Euphorbia tortilis cactus as a natural additive", *Matéria (Rio de Janeiro)*, v. 28, n. 1, pp. e20220233, 2023. doi: <http://dx.doi.org/10.1590/1517-7076-rmat-2022-0233>.

- [4] NGUYEN, T.H.Y., TRAN, V.M., PANSUK, W., *et al.*, “Electrochemical chloride extraction on reinforced concrete contaminated external chloride: efficiencies of intermittent applications and impacts on hydration products”, *Cement and Concrete Composites*, v. 121, pp. 104076, 2021. doi: <http://dx.doi.org/10.1016/j.cemconcomp.2021.104076>.
- [5] SHI, X., XIE, N., FORTUNE, K., *et al.*, “Durability of steel reinforced concrete in chloride environments: an overview”, *Construction & Building Materials*, v. 30, pp. 125–138, 2012. doi: <http://dx.doi.org/10.1016/j.conbuildmat.2011.12.038>.
- [6] ALLISON, P.G., MOSER, R.D., CHANDLER, M.Q., *et al.*, *Electro Migration and deposition of Microscale Calcium Carbonate structure with controlled Morphology and Polymorphism*, US, Engineering Research and Development Centre, 2013.
- [7] SHARIF, A., “Review on advances in nanoscale microscopy in cement research”, *Micron (Oxford, England)*, v. 80, pp. 45–58, 2016. doi: <http://dx.doi.org/10.1016/j.micron.2015.09.010>. PubMed PMID: 26447783.
- [8] YANG, Y., WANG, M., “Pore-scale modeling of chloride ion diffusion in cement microstructures”, *Cement and Concrete Composites*, v. 85, pp. 92–104, 2018. doi: <http://dx.doi.org/10.1016/j.cemconcomp.2017.09.014>.
- [9] MOREFIELD, S.W., HOCK, V.F., WEISS, C.A., *et al.*, *Application of electrokinetic nanoparticle migration in the production of novel concrete-based composites*, Arlington, US Army Office of the Assistant Secretary, 2008.
- [10] KUPWADE-PATIL, K., JOHN, T.J., MATHEW, B., *et al.*, “Diffusion analysis of chloride in concrete following electrokinetic nanoparticle treatment”, In: *International Conference on Nanochannels, Microchannels, and Minichannels*, pp. 305–312, 2010. doi: <http://dx.doi.org/10.1115/FEDSM-ICNMM2010-31153>.
- [11] CARDENAS, H., KUPWADE-PATIL, K., EKLUND, S., “Corrosion mitigation in mature reinforced concrete using nanoscale pozzolan deposition”, *Journal of Materials in Civil Engineering*, v. 23, n. 6, pp. 752–760, 2011. doi: [http://dx.doi.org/10.1061/\(ASCE\)MT.1943-5533.0000194](http://dx.doi.org/10.1061/(ASCE)MT.1943-5533.0000194).
- [12] KAMRAN, K., VAN SOESTBERGEN, M., HUININK, H.P., *et al.*, “Inhibition of electrokinetic ion transport in porous materials due to potential drops induced by electrolysis”, *Electrochimica Acta*, v. 78, pp. 229–235, 2012. doi: <http://dx.doi.org/10.1016/j.electacta.2012.05.123>.
- [13] DEPAOLI, D.W., HARRIS, M.T., MORGAN, I.L., *et al.*, “Investigation of electrokinetic decontamination of concrete”, *Separation Science and Technology*, v. 32, n. 1–4, pp. 387–404, 1997. doi: <http://dx.doi.org/10.1080/01496399708003205>.
- [14] KIM, C., CHOI, S., SHIN, M., “Review: Electro-kinetic decontamination of radioactive concrete waste from nuclear power plants”, *Journal of the Electrochemical Society*, v. 16, n. 9, pp. E330–E344, 2018. doi: <http://dx.doi.org/10.1149/2.0281809jes>.
- [15] WIECZOREK, S., WEIGAND, H., SCHMID, M., *et al.*, “Electrokinetic remediation of an electroplating site: design and scale-up for an in-situ application in the unsaturated zone”, *Engineering Geology*, v. 77, n. 3-4, pp. 203–215, 2005. doi: <http://dx.doi.org/10.1016/j.enggeo.2004.07.011>.
- [16] SANDEEP, M. S., TIPRAK, K., KAEWUNRUEN, S., *et al.* “Shear strength prediction of reinforced concrete beams using machine learning”. *Structures*. v. 47, pp. 1196–1211, 2023. <https://doi.org/10.1016/j.istruc.2022.11.140>
- [17] YEGANEH, M., OMIDI, M., MORTAZAVI, H., *et al.* “Enhancement routes of corrosion resistance in the steel reinforced concrete by using nanomaterials”, In: Liew, M.S., Nguyen-Tri, P., Nguyen, T.A., *et al.* (eds), *Smart nanoconcretes and cement-based materials*, Amsterdam, Elsevier, 2020, pp. 583–599. doi: <http://dx.doi.org/10.1016/B978-0-12-817854-6.00026-X>.
- [18] RANJITHA, K., MANJARI BLESSING, B.V., “Soil stabilization by Electro Kinetic method”, *International Journal of Scientific Research*, v. 6, n. 2, 2017.
- [19] CARDENAS, H., KUPWADE-PATIL, K., EKLUND, S., “Recovery from sulfate attack in concrete via electrokinetic nanoparticle treatment”, *Journal of Materials in Civil Engineering*, v. 23, n. 7, pp. 1103–1112, 2011. doi: [http://dx.doi.org/10.1061/\(ASCE\)MT.1943-5533.0000255](http://dx.doi.org/10.1061/(ASCE)MT.1943-5533.0000255).
- [20] ARUTZELVAM, A., “Soft clay stabilization using electro kinetic process”, *International Journal on Engineering Technology and Sciences*, v. 1, n. 2, pp. 50–55, 2014.

- [21] HSIEH, C., WU, J.H., LU, X.J., “Electro-kinetic techniques and geotextiles for high water content sludge dehydration tests.”, *Japanese Geotechnical Society Special Publication*, v. 2, n. 65, pp. 2221–2225, 2016. doi: <http://dx.doi.org/10.3208/jgssp.IGS-05>.
- [22] ARTIALOK, R.P., TIWARI, R.P., SINGH, R.P., “Effect of Ph of anolyte in electro kinetic remediation of cadmium contaminated soil”, *International Journal of Engineering Research & Technology (Ahmedabad)*, v. 1, n. 10, pp. 1–11, 2012.
- [23] KUPWADE-PATIL, K., “Mitigation of chloride and sulfate-based corrosion in reinforced concrete via electrokinetic nanoparticle treatment”, M.Sc. Thesis, Louisiana Tech University, Unites States, 2010.
- [24] AKTER, J., HANIF, M.A., ISLAM, M.A., *et al.*, “Visible-light-active novel α -Fe₂O₃/Ta₃N₅ photocatalyst designed by band-edge tuning and interfacial charge transfer for effective treatment of hazardous pollutants”, *Journal of Environmental Chemical Engineering*, v. 9, n. 6, pp. 106831, 2021. doi: <http://dx.doi.org/10.1016/j.jece.2021.106831>.
- [25] KUPWADE-PATIL, K., JOHN, T.J., MATHEW, B., *et al.*, “Diffusion analysis of chloride in concrete following electrokinetic nanoparticle treatment”, In: *International Conference on Nanochannels, Microchannels, and Minichannels*, pp. 305–312, 2010. doi: <http://dx.doi.org/10.1115/FEDSM-ICNMM2010-31153>.
- [26] ABUSHANAB, A., ALNAHHAL, W., “Combined effects of treated domestic wastewater, fly ash, and calcium nitrite toward concrete sustainability”, *Journal of Building Engineering*, v. 44, pp. 103240, 2021. doi: <http://dx.doi.org/10.1016/j.jobbe.2021.103240>.
- [27] ETIM, I.I.N., DONG, J., WEI, J., *et al.*, “Mitigation of sulphate-reducing bacteria attack on the corrosion of 20SiMn steel rebar in sulphoaluminate concrete using organic silicon quaternary ammonium salt”, *Construction & Building Materials*, v. 257, pp. 119047, 2020. doi: <http://dx.doi.org/10.1016/j.conbuildmat.2020.119047>.
- [28] OTTOSEN, L.M., CHRISTENSEN, I.V., RÖRIG-DALGÅRD, I., *et al.*, “Utilization of electromigration in civil and environmental engineering—processes, transport rates and matrix changes”, *Journal of Environmental Science and Health. Part A, Toxic/Hazardous Substances & Environmental Engineering*, v. 43, n. 8, pp. 795–809, 2008. doi: <http://dx.doi.org/10.1080/10934520801973949>. PubMed PMID: 18569289.
- [29] INDIAN STANDARD, *Methods of sampling and test (physical and chemical) for water and wastewater*, New Delhi, IS, 2006.
- [30] MATYŠČÁK, O., OTTOSEN, L.M., RÖRIG-DALGAARD, I., “Desalination of salt damaged Obernkirchen sandstone by an applied DC field”, *Construction & Building Materials*, v. 71, pp. 561–569, 2014. doi: <http://dx.doi.org/10.1016/j.conbuildmat.2014.08.051>.
- [31] VELUMANI, M., MOHANRAJ, R., KRISHNASAMY, R., *et al.*, “Durability evaluation of cactus-infused M25 grade concrete as a bio-admixture”, *Periodica Polytechnica. Civil Engineering*, n. June, 2023. doi: <http://dx.doi.org/10.3311/PPci.22050>.
- [32] ROTTA LORIA, A.F., SHIROLE, D., VOLPATTI, G., *et al.*, “Engineering concrete properties and behavior through electrodeposition: a review”, *Journal of Applied Electrochemistry*, v. 53, n. 2, pp. 193–215, 2023. doi: <http://dx.doi.org/10.1007/s10800-022-01770-2>.
- [33] POPOV, K., GLAZKOVA, I., YACHMENEV, V., *et al.*, “Electrokinetic remediation of concrete: effect of chelating agents”, *Environmental Pollution*, v. 153, n. 1, pp. 22–28, 2008. doi: <http://dx.doi.org/10.1016/j.envpol.2008.01.014>. PubMed PMID: 18313182.
- [34] MOHANRAJ, R., SENTHILKUMAR, S., GOEL, P., *et al.*, “A state-of-the-art review of Euphorbia Tortilis cactus as a bio-additive for sustainable construction materials”, *Materials Today: Proceedings*, 2023. In press. doi: <http://dx.doi.org/10.1016/j.matpr.2023.03.762>.
- [35] JIANG, C., SONG, C., GU, X.L., *et al.*, “Modeling electrochemical chloride extraction process in cement-based materials considering coupled multi-ion transports and thermodynamic equilibriums”, *Journal of Cleaner Production*, v. 401, pp. 136778, 2023. doi: <http://dx.doi.org/10.1016/j.jclepro.2023.136778>.
- [36] ZHU, Z., CHU, H., GUO, M.Z., *et al.*, “Anti-microbial corrosion performance of concrete treated by Cu₂O electrodeposition: Influence of different treatment parameters”, *Cement and Concrete Composites*, v. 123, pp. 104195, 2021. doi: <http://dx.doi.org/10.1016/j.cemconcomp.2021.104195>.
- [37] LOGANATHAN, P., MOHANRAJ, R., SENTHILKUMAR, S., *et al.*, “Mechanical performance of ETC RC beam with U-framed AFRP laminates under a static load condition.”, *Revista de la Construcción*, v. 21, n. 3, pp. 679–691, 2022. doi: <http://dx.doi.org/10.7764/RDLC.21.3.678>.

- [38] SALIH, M., AHMED, S. “Mix design for sustainable high strength concrete by using ggbs and micro silica as supplementary cementitious materials”, *International Review of Civil Engineering*, v. 11, n. 1, pp. 45, 2020. doi: <http://dx.doi.org/10.15866/irece.v11i1.17784>.
- [39] SALIH, M.A., AHMED, S.K., ALSAFI, S., *et al.*, “Strength and durability of sustainable self-consolidating concrete with high levels of supplementary cementitious materials”, *Materials (Basel)*, v. 15, n. 22, pp. 7991, 2022. doi: <http://dx.doi.org/10.3390/ma15227991>. PubMed PMID: 36431478.